Phytomedicine 76 (2020) 153264

Contents lists available at ScienceDirect

Phytomedicine

journal homepage: www.elsevier.com/locate/phymed

Effects of 23-epi-26-deoxyactein on adipogenesis in 3T3-L1 preadipocytes and diet-induced obesity in C57BL/6 mice

Jingjing Yuan[a], Qiangqiang Shi[b], Juan Chen[a], Jing Lu[b], Lu Wang[a], Minghua Qiu[b,**], Jian Liu[a,c,*]

[a] School of Biotechnology and Food Engineering, Hefei University of Technology, Hefei 230009, China
[b] State Key Laboratory of Phytochemistry and Plant Resources in West China, Kunming Institute of Botany, Chinese Academy of Sciences, Kunming 650201, China
[c] Engineering Research Center of Bio-process, Ministry of Education, Hefei University of Technology, Hefei 230009, China

ARTICLE INFO

Keywords:
23-epi-26-deoxyactein
Actaea racemosa L.
Adipogenesis
Diet-induced obesity
Lipolysis

ABSTRACT

Background: The ethanolic extract of *Actaea racemosa* L. (*Cimicifuga racemosa* (L.) Nutt.) has recently been reported to ameliorate obesity-related insulin resistance, hyperlipidemia, and fatty liver in rodents. However, it remains unclear which *A. racemosa* components are responsible for these beneficial effects.

Purpose: We aimed to examine the anti-obesity potential of 23-epi-26-deoxyactein (DA), which is contained in the ethanolic extracts of *A. racemosa*.

Study design and methods: To evaluate the effects of DA on adipogenesis in 3T3-L1 preadipocytes and diet-induced obesity in C57BL/6 mice, *in vitro* and *in vivo* tests were performed. For *in vitro* assessment, we used Oil red O staining that showed lipid accumulation in differentiated 3T3-L1 cells. For *in vivo* tests, male 5-week-old C57BL/6 mice were fed with low-fat diet (LFD), high-fat diet (HFD), HFD with 10 mg/kg/d luteolin (LU; positive control drug), HFD with 1 mg/kg/d DA, and HFD with 5 mg/kg/d DA for 12 weeks, respectively. Glucose and insulin tolerance tests were performed at week 17. The lipid deposition of adipose tissue and liver was visualized by hematoxylin and eosin staining. Real-time PCR showed mRNA levels of genes involved in adipogenesis, lipogenesis, and lipolysis. AMPK signaling and SIRT1-FOXO1 pathway were assessed by real-time PCR and western blot.

Results: 10 μM DA and 20 μM LU treatments inhibited 3T3-L1 adipogenesis through down-regulating the expression of *C/ebpα, C/ebpβ*, and *Pparγ*, which are the critical adipogenic transcription factors. The *in vivo* results showed that 5 mg/kg/d DA and 10 mg/kg/d LU significantly lowered body weight gain, fat mass, and liver weight in HFD-fed mice. Meanwhile, DA and LU also reduced insulin resistance and serum lipoprotein levels in HFD-fed mice. Mechanistic studies showed that DA and LU promoted adipocyte lipolysis in mice through activating the AMPK signaling and SIRT1-FOXO1 pathway.

Conclusion: The *in vitro* results indicate that 10 μM DA suppresses adipogenesis in 3T3-L1 preadipocytes. The *in vivo* treatment with 5 mg/kg/d DA ameliorates diet-induced obesity in mice, suggesting that DA is a promising natural compound for the treatment of obesity and related metabolic diseases.

Introduction

Obesity is a multifactorial chronic disease that is associated with the increased risks of type 2 diabetes, hyperlipidemia, and nonalcoholic fatty liver diseases (Bornfeldt and Tabas, 2011). In 2016, the World Health Organization estimated that more than 650 million adults and 124 million children were obese (World Health Organization, 2020; NCD Risk Factor Collaboration, 2017). It is predicted that there will be

Abbreviations: ALT, alanine aminotransferase; AMPK, AMP-activated protein kinase; AST, aspartate aminotransferase; ATGL, adipose triglyceride lipase; BAT, brown adipose tissue; C/EBPα, CCAAT/enhancer-binding protein α; C/EBPβ, CCAAT/enhancer-binding protein β; DA, 23-epi-26-deoxyactein; DGAT1, diacylglycerol acyltransferase-1; DGAT2, diacylglycerol acyltransferase-2; EAT, epididymal adipose tissue; FOXO1, forkhead transcription factor O1; GPAT3, glycerol-3-phosphate acyltransferase-3; GTT, glucose tolerance test; HDL-C, high-density lipoprotein cholesterol; H&E, hematoxylin and eosin; HFD, high-fat diet; HSL, hormone-sensitive lipase; ITT, insulin tolerance test; LDL-C, low-density lipoprotein cholesterol; LFD, low-fat diet; LU, luteolin; MOGAT2, monoacylglycerol acyltransferase-2; PPARγ, peroxisome proliferator-activated receptor γ; SAT, subcutaneous adipose tissue; SIRT1, sirtuin1; TC, total cholesterol; TG, triglycerides

* Corresponding author at: School of Biotechnology and Food Engineering, Hefei University of Technology, 193 Tunxi Road, Hefei, Anhui 230009, China.
** Co-corresponding author at: State Key Laboratory of Phytochemistry and Plant Resources in West China, Kunming Institute of Botany, Chinese Academy of Sciences, Kunming 650204, China.
E-mail addresses: mhchiu@mail.kib.ac.cn (M. Qiu), liujian509@hfut.edu.cn (J. Liu).

https://doi.org/10.1016/j.phymed.2020.153264
Received 20 August 2019; Received in revised form 23 April 2020; Accepted 3 June 2020

1.12 billion obese people in the world by 2030 (Kelly et al., 2008). Given the established health risks and increasing prevalence, there is an urgent need for new strategies in the treatment of obesity.

Adipose tissue plays a critical role in the development of obesity. Obesity is associated with both adipocyte hypertrophy (enlargement in cell size) and hyperplasia (increase in cell number) of adipose tissue (Cristancho and Lazar, 2011; Wang et al., 2013). At the cellular level, the former is determined by lipogenesis while the latter by adipogenesis. Lipogenesis refers to the lipid accumulation and enlarged size of differentiated adipocytes (Cristancho and Lazar, 2011). Adipogenesis represents the recruitment and proliferation of preadipocytes, followed by their subsequent differentiation into mature fat cells (Wang et al., 2013). In addition, the intracellular triglyceride can be mobilized through lipolysis to provide fatty acids (FAs) that are used as energy substrates when there is an energy shortage (Zechner et al., 2012). Thus, the natural extracts inhibiting adipogenesis, suppressing lipogenesis, and promoting lipolysis have been recommended to combat obesity and associated metabolic diseases (Chang and Kim, 2019; Hsieh and Wang, 2013).

Actaea racemosa L. (Ranunculaceae) (synonim *Cimicifuga racemosa* (L.) Nutt.; common name "black cohosh") is widely used as an alternative treatment of menopause-related symptoms in the United States and Europe. As a herbal medicinal product, its effectiveness and safety have been clinically confirmed over 10 years (Committee on Herbal Medicinal Products, 2018). It was recently shown that the isopropanolic extract from *A. racemosa* rhizomes reduced ovariectomy-induced body weight gain, adipocyte hypertrophy, and hepatic fat accumulation in rats (Sun et al., 2016). Additionally, a short-term study showed that Ze 450, an ethanolic extract of *A. racemosa* rhizomes, significantly decreased body weight gain and improved insulin sensitivity in *ob/ob* mice (Moser et al., 2014). However, it is not clear which active compounds from *A. racemosa* extracts contribute to the beneficial effects. As a chemical marker in *A. racemosa*, 23-epi-26-deoxyactein (DA) is contained (in 6–15% of the total triterpene glycosides) in the ethanolic extracts of *A. racemosa* (Masada-Atsumi et al., 2014; Wang et al., 2005). Recently, it has been reported that DA promotes mitochondrial biogenesis in pancreatic β-cells preventing methylglyoxal-induced oxidative cell damage (Suh et al., 2017), inhibits the growth of breast cancer cells (Einbond et al., 2004) and protects osteoblasts against antimycin A-induced cell damage (Choi, 2013). However, it remains unknown whether DA affects adipocyte adipogenesis, lipogenesis, or lipolysis.

In this study, we firstly investigated the antiadipogenic effect of DA in 3T3-L1 preadipocytes. Further, we tested whether DA could ameliorate obesity and associated metabolic alterations in HFD-fed mice. Finally, the impacts of DA on adipose tissue lipogenesis and lipolysis were also examined in the mice.

Materials and methods

Materials

DA was extracted and purified from *A. racemosa*. Briefly, 1 kg dried and milled roots of *A. racemosa* were extracted with 95% EtOH (3 × 5 h) at room temperature. After evaporating under vacuum at 50 ˚C, the residue was suspended in H_2O. The aqueous suspension was then extracted with EtOAc to give an EtOAc fraction. The EtOAc extract (50 g) was chromatographed over a silica gel column and eluted with $CHCl_3-MeOH$ (100:0, 50:1, 20:1, 10:1) to obtain four fractions (A-D). Fraction C was subjected to column chromatography on ODS silica gel and eluted with $MeOH-H_2O$ (4:6, 5:5, 6:4, 7:3, 8:2, 9:1) to obtain six fractions (C-1, C-2, C-3, C-4, C-5, and C-6). Further, fraction C-4 was chromatographed over a silica gel column with $CHCl_3-MeOH$ (30:1, 25:1, 20:1, 15:1, 10:1) to obtain five fractions (C-4-1, C-4-2, C-4-3, C-4-4, and C-4-5). Finally, DA (500 mg) was isolated and purified from fraction C-4-3 by silica gel column and semi-preparative HPLC (CH_3CN-H_2O, 68:32, t_R = 15, 3 min). Its chemical structure was confirmed by NMR spectrum analyses, and the NMR data was presented in Supplementary file 1. The purity of DA showed to be ≥ 98% by ^1H and ^{13}C NMR spectra (Supplementary material Fig 1). Luteolin (LU; purity ≥ 98%, Huayi Biotechnology, Shanghai, China), which can inhibit adipogenesis in 3T3-L1 cells and diet-induced obesity in mice (Kwon et al., 2015; Park et al., 2009; Zhang et al., 2016), was used as the positive drug in both *in vitro* and *in vivo* studies.

Cell culture, cytotoxic assessment, and differentiation of 3T3-L1 preadipocytes

The 3T3-L1 preadipocytes were obtained from Cell Culture Center of Peking Union Medical College, and cells were cultured in high glucose Dulbecco's modified Eagle's medium (Gibco, Auckland, New Zealand) containing 10% FBS and 1% penicillin and streptomycin. DA was dissolved in dimethyl sulfoxide (Sigma-Aldrich, Shanghai, China), and then was diluted with Dulbecco's modified Eagle's medium to the indicated concentrations. Cell cytotoxicity assay was performed as previously described (Hsu and Yen, 2007). For the adipogenesis of 3T3-L1 preadipocytes, cells were induced by the differentiation cocktail (Park et al., 2009). 0.1, 1, 5, 10, 20, or 50 μM DA was added during 3T3-L1 differentiation. On day 8 of differentiation, lipid droplet accumulation in the differentiated cells was visualized by Oil red O staining. The Oil red O dye in fat droplets was dissolved in anhydrous ethanol, and absorbances at 510 nm were then measured in ELx800 microplate reader (Bio-Tek Industries, Inc., Atlanta, GA, USA).

In vivo studies

All animal experiments were approved by the Standing Committee on Animals of Hefei University of Technology (permission number: 20170811-01). Male 3-week-old C57BL/6 mice were obtained from Vital River Laboratory Animal Technology Co. Ltd. (Beijing, China). Mice were maintained in a barrier facility, at room temperature, on a regular 12-h light and 12-h dark cycle with *ad libitum* access to food and water. Male 5-week-old C57BL/6 mice were fed on low-fat diet (LFD; 10% of calories derived from fat, Research Diets, D12450B), high-fat diet (HFD; 45% of calories derived from fat, Research Diets, D12451), HFD with 10 mg/kg/d LU, HFD with 1 mg/kg/d DA, and HFD with 5 mg/kg/d DA for 12 weeks, respectively. The detailed composition of all diets was shown in Supplementary material Table 1. The body weight and food intake of mice were measured weekly. Glucose tolerance tests (GTT) and insulin tolerance tests (ITT) were performed in 17-week-old mice according to the published methods (Xu et al., 2014). Mice were sacrificed with CO_2. Serum samples, liver, epididymal adipose tissue (EAT), subcutaneous adipose tissue (SAT), and brown adipose tissue (BAT) were harvested. Serum triglyceride (TG), total cholesterol (TC), high-density lipoprotein cholesterol (HDL-C), low-density lipoprotein cholesterol (LDL-C), aspartate aminotransferase (AST) and alanine aminotransferase (ALT) were examined using an automatic biochemistry analyzer (Beckman Coulter, Brea, CA, USA).

Hematoxylin and eosin (H&E) staining

Tissues were fixed, dehydrated, embedded, and serially sliced at 5 μm thickness for H&E staining. The sections were deparaffinized, rehydrated, and stained with H&E using standard protocols. Five random fields from each section were evaluated, and adipocyte average diameters were measured using Image-Pro Plus Version 6.0 (Media Cybernetics, Bethesda, MD, USA).

RNA extraction, cDNA synthesis, and quantitative real-time PCR

Total RNA was extracted from 3T3-L1 cells and adipose tissue using RNAiso Plus reagent (Takara, Osaka, Japan) according to the manufacturer's instructions. The RNA quality and quantity were evaluated

using a spectrophotometer (Thermo Fisher Scientific, Waltham, MA, USA). RNA purity was assessed at an absorbance OD ratio of 260/280. Total RNA (1 μg) was reverse-transcribed into cDNA using a reverse transcription kit (Takara) according to the manufacturer's instructions. Quantitative real-time PCR was performed using SYBR® Premix Ex Taq™ II (Takara) on a real-time fluorescent quantitative PCR analyzer (Bio-Rad, Hercules, CA, USA). All primer sequences used were listed in Supplementary material Table 2. Quantitative real-time PCR reactions were initiated by denaturation at 95 °C for 3 min, followed by 35 cycles of amplification (95 °C for 10 s, 60 °C for 20 s). The $2^{-\Delta\Delta CT}$ method was used to analyze the relative changes in gene expression normalized against *β*-actin mRNA expression.

Total protein extraction and immunoblotting

Tissues were homogenized, lysed, and centrifuged at 12,000 g for 30 min at 4 °C. The supernatant was then collected. The protein concentration of the supernatant was determined using a BCA assay kit (Sangon, Shanghai, China). Proteins were separated on the SDS-polyacrylamide gel and transferred onto a polyvinylidene difluoride membrane (Millipore, Bedford, MA, USA). The membrane was blocked for 2 h and was then incubated with a primary antibody. Primary antibodies were listed in Supplementary material Table 3. Then, the membrane was incubated with HRP-labeled goat anti-rabbit IgG (1:5000; Cell Signaling Technology, Danvers, MA, USA) for 2 h. The protein bands were detected and analyzed using the ECL kit (Thermo, Rockford, IL, USA) and Image Quant LAS 4000 mini (GE Healthcare, Shanghai, China). Signal intensities were quantified using Image Quant TL 7.0 software (GE Healthcare).

Statistical analysis

All data were analyzed using SPSS 16.0 and presented as means ± SEM. Figures were prepared using Origin 9.0. For cell studies, statistical significance was calculated by the unpaired student's *t*-test. For animal studies, the nonparametric Mann-Whitney U test was used. $p < 0.05$ was considered as statistical significance.

Results

Effects of DA on adipogenesis in 3T3-L1 preadipocytes

To investigate the effect of DA on adipogenesis, we firstly evaluated the cytotoxicity of DA (Fig. 1A) on 3T3-L1 preadipocytes. The results showed that DA did not inhibit cell viability, even at 50 μM (Fig. 1B). Further, we examined the antiadipogenic effects of DA at 0.1, 1, 5, 10, 20, and 50 μM in 3T3-L1 preadipocytes. Oil red O staining showed that DA significantly inhibited the differentiation and lipid accumulation of 3T3-L1 preadipocytes in a dose-dependent manner (Fig. 1C and D), suggesting a potent anti-adipogenic activity of DA.

Effects of DA on the different stages of 3T3-L1 differentiation

Adipogenesis of 3T3-L1 preadipocyte is a multiple-step process. The conversion of preadipocytes into adipocytes involves the early, intermediate, and late stages of differentiation (Ntambi and Young-Cheul, 2000). To find out which stages of 3T3-L1 differentiation were inhibited by DA, we set up 7 groups according to the duration of DA (10 μM) treatment, as indicated in Fig. 2A. In groups 1, 2, 3, or 4, DA was added during 0–2, 0–4, 0–6, or 0–8 days of 3T3-L1 differentiation and significantly suppressed the adipogenic levels (Fig. 2B and C). While in groups 5, 6, or 7, DA was added during 2–8, 4–8, or 6–8 days of 3T3-L1 differentiation and unaffected lipid accumulation (Fig. 2B and C). These results indicate that 10 μM DA inhibits the adipogenesis of 3T3-L1 preadipocytes mainly at the early stage of differentiation.

CCAAT/enhancer-binding protein *β* (C/EBP*β*), peroxisome proliferator-activated receptor γ (PPARγ), and CCAAT/enhancer-binding protein *α* (C/EBP*α*), which are activated during 3T3-L1 preadipocyte differentiation, transcriptionally regulate multiple adipogenesis-related genes (Ntambi and Young-Cheul, 2000; Tang and Lane, 2012). To further elucidate the mechanism underlying DA-inhibited adipogenesis, we monitored the expression of *C/ebpβ, Pparγ*, and *C/ebpα* during 3T3-L1 differentiation. Supporting the results of Oil red O staining (Fig. 2B and C), the mRNA expression of *C/ebpβ, Pparγ*, and *C/ebpα* were significantly suppressed by 10 μM DA since the 2nd day of differentiation (Fig. 2D-F). These results demonstrate that 10 μM DA represses 3T3-L1 preadipocyte adipogenesis through down-regulating the expression of the critical adipogenic transcription factors.

Effects of DA on diet-induced obesity in mice

The anti-adipogenic activity of DA in 3T3-L1 preadipocytes suggests its potential anti-obesity function *in vivo*. To assess the effect of DA on diet-induced obesity, we randomly grouped 5-week-old C57BL/6 mice into 5 groups as LFD, HFD, HFD + 10 mg/kg/d LU, HFD + 1 mg/kg/d DA, and HFD + 5 mg/kg/d DA. After a 12-week treatment, HFD-fed mice gained more body weight (Fig. 3A) and fat mass (Fig. 3C) than LFD-fed controls. Encouragingly, 5 mg/kg/d DA treatment significantly attenuated diet-induced body weight (Fig. 3A) and fat mass gain (Fig. 3C) without affecting energy intake (Fig. 3B), although 1 mg/kg/d DA could not reduce the body weight gain (Fig. 3A). Additionally, H&E staining of EAT, SAT, and BAT sections showed that 5 mg/kg/d DA strikingly reduced lipid deposition (Fig. 3D) and adipocyte size (Fig. 3E) in HFD-fed mice. These results indicate that 5 mg/kg/d DA effectively reduces diet-induced obesity in mice.

Effects of DA on obesity-related metabolic disorders in HFD-fed mice

Obesity is a modern disease associated with many metabolic alterations (Bornfeldt and Tabas, 2011). Here, we next investigated the effects of DA on obesity-associated metabolic phenotypes, such as insulin resistance, fatty liver, and hyperlipidemia. Firstly, GTT and ITT showed that 5 mg/kg/d DA significantly improved HFD-induced glucose intolerance (Fig. 4A) and insulin resistance (Fig. 4B). Along with their lower liver weights (Fig. 4C), the mice treated with DA also had lower liver lipid deposition (Fig. 4D). Accordingly, DA significantly reduced serum AST and ALT levels in HFD-fed mice (Fig. 4E). Moreover, compared to HFD-fed controls, the mice fed with DA-containing HFD also had decreased serum levels of HDL-C, LDL-C, TC, and TG (Fig. 4F). Altogether, these findings demonstrate that DA can ameliorate obesity-related insulin resistance, hepatic lipid accumulation, and hyperlipidemia.

Effects of DA on lipogenesis and lipolysis in adipose tissue

The level of adipose tissue triglyceride (TG) can be impacted by lipogenesis and lipolysis (Coleman and Mashek, 2011). The imbalance between adipose tissue lipogenesis and lipolysis plays a vital role in the development of obesity and associated metabolic diseases (Sam and Mazzone, 2014). Therefore, to explore the potential mechanisms by which DA reduced the HFD-induced obesity in mice, we next examined the expression of genes involved in lipolysis and lipogenesis. The process of lipolysis includes three consecutive steps, with different enzymes at each step. Adipose triglyceride lipase (ATGL) and hormone-sensitive lipase (HSL) are two key enzymes catalyzing lipolysis (Zechner et al., 2012). Perilipin has emerged as an essential mediator of stimulated lipolysis (Frühbeck et al., 2014). Significantly, the expression levels of *Atgl, Hsl,* and *perilipin* in adipose tissue were down-regulated by HFD. However, DA strikingly increased their mRNA levels in HFD-fed mice (Fig. 5A).

The biosynthesis of TG can be catalyzed by several key enzymes, including monoacylglycerol acyltransferase-2 (MOGAT2),

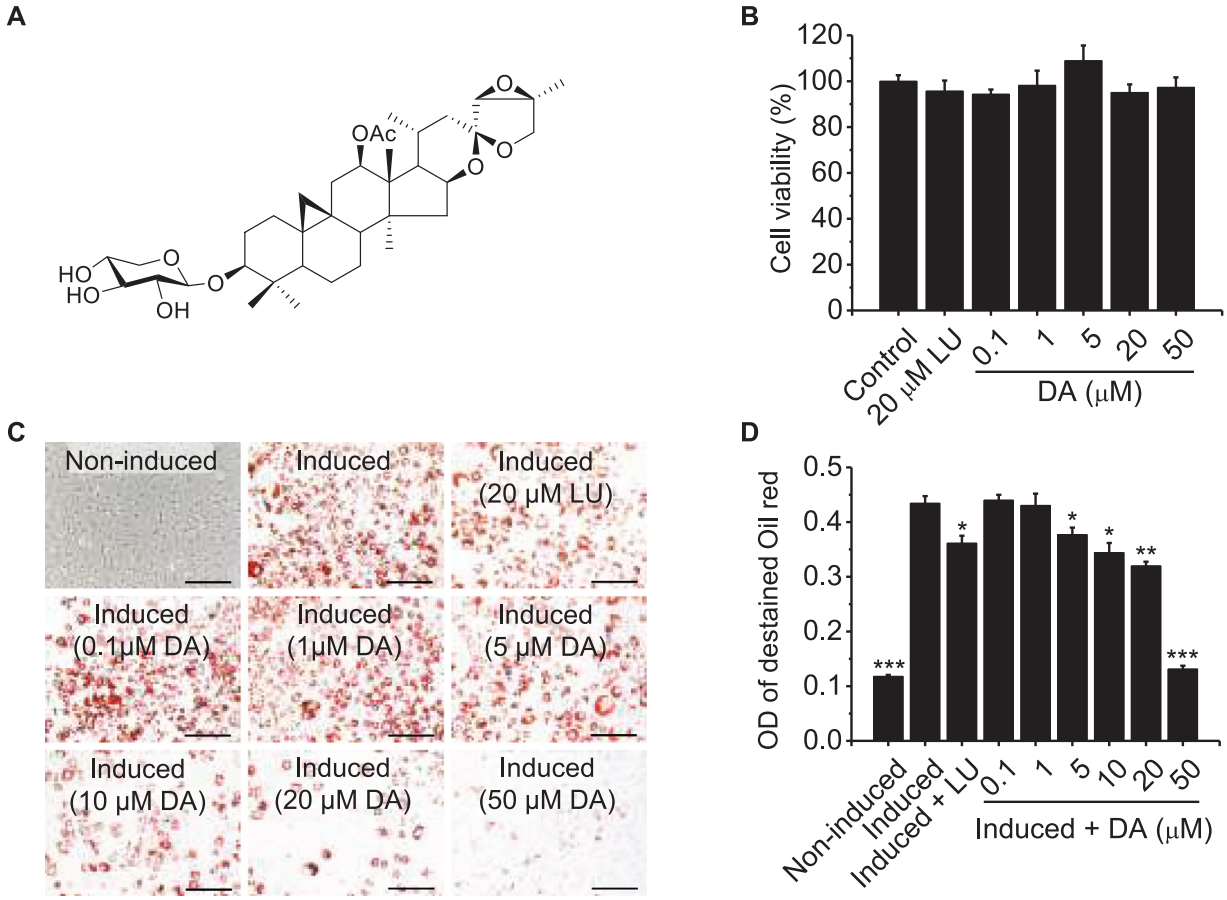

Fig. 1. Effects of DA on adipogenesis in 3T3-L1 preadipocytes. (A) The chemical structure of 23-epi-26-deoxyactein (DA). (B) Cell viability assay of DA in 3T3-L1 preadipocytes ($n = 5$). (C) Oil red O staining of lipid accumulation in differentiated adipocytes. Scale bar, 100 μm. (D) The quantification of Oil red O staining in 3T3-L1 adipocytes ($n = 4$). All data in (B, D) are represented as mean ± SEM. Statistical difference was determined by Student's *t*-test, * $p < 0.05$, ** $p < 0.01$, *** $p < 0.001$. LU, luteolin.

diacylglycerol acyltransferase-1 (DGAT1), diacylglycerol acyltransferase-2 (DGAT2), and glycerol-3-phosphate acyltransferase-3 (GPAT3) (Coleman and Mashek, 2011). We observed that HFD-induced reduction of *Dgat1* expression was reversed by DA (Fig. 5B). HFD control mice and the mice fed with DA-containing HFD had similar mRNA levels of *Dgat2* and *Mogat2* to LFD-fed mice (Fig. 5B). In addition, although *Gpat3* expression in adipose tissue was not affected by HFD, DA upregulated the mRNA level of *Gpat3* in HFD-fed mice (Fig. 5B). Together, these results demonstrate that DA improves diet-induced obesity and abnormal metabolic alterations through activating adipocyte lipolysis, rather than inhibiting adipocyte lipogenesis.

Effects of DA on AMPK signaling and SIRT1-FOXO1 pathway

ATGL, the critical initial lipase in adipocyte lipolysis, can be activated by either AMP-activated protein kinase (AMPK) or sirtuin1 (SIRT1)-mediated deacetylation of forkhead transcription factor O1 (FOXO1) (Ahmadian et al., 2011; Chakrabarti et al., 2011). To further understand the mechanisms underlying DA-induced lipolysis, we detected the expression of SIRT1, FOXO1, and AMPK*α*1 in adipose tissue. The mRNA levels of *Sirt1, Foxo1*, and *Ampkα1* in HFD-fed mice were significantly lower than those in LFD-fed mice (Fig. 6A). In contrast, DA markedly increased the expression of *Sirt1, Foxo1*, and *Ampkα1* in HFD-fed mice (Fig. 6A). Consistent with the changes in the mRNA expression, DA also significantly elevated the protein levels of SIRT1, FOXO1, and ATGL, as well as the phosphorylation of AMPK*α*1 in adipose tissue (Fig. 6B and C). These results suggest that DA activates AMPK signaling and SIRT1-FOXO1 pathway to enhance ATGL expression and hence promotes adipose tissue lipolysis in HFD-fed mice.

Discussion

Globally, dietary change is an important cause in the rising rates of obesity, which is a significant risk factor for diabetes, fatty liver, and hyperlipidemia (Bornfeldt and Tabas, 2011). Therefore, the appropriate use of herbal medicinal products, which possess anti-obesity activities, is expected to ameliorate obesity and associated metabolic diseases. This study showed the inhibition of DA on adipogenesis in 3T3-L1 preadipocytes and diet-induced obesity in mice.

Recent studies have demonstrated that DA-containing *A. racemosa* extracts could reduce body weight gain and improve insulin sensitivity in menopausal and genetic obese animal models (Moser et al., 2014; Rachoń et al., 2008; Sun et al., 2016). In the study, DA significantly inhibited the differentiation of 3T3-L1 preadipocytes at 5–50 μM. According to the DA concentration range, we used 1 mg/kg/d and 5 mg/kg/d DA to evaluate the effect of DA on diet-induced obesity in mice. The results showed that 5 mg/kg/d DA effectively ameliorated obesity in HFD-fed mice. Thus, we speculate that DA may have substantial anti-obesity properties and may also improve menopausal and genetic obesity and associated metabolic syndromes.

The development of obesity is accompanied by the expansion of adipose tissue. During HFD challenges, adipose depots can expand through adipocyte hyperplasia (*i.e.*, adipogenesis) and hypertrophy (*i.e.*, lipogenesis). Meanwhile, HFD-induced decline in lipolysis level also contributes to adipose tissue expansion (Coleman and Mashek, 2011; Wang et al., 2013). Accordingly, in the present study, we

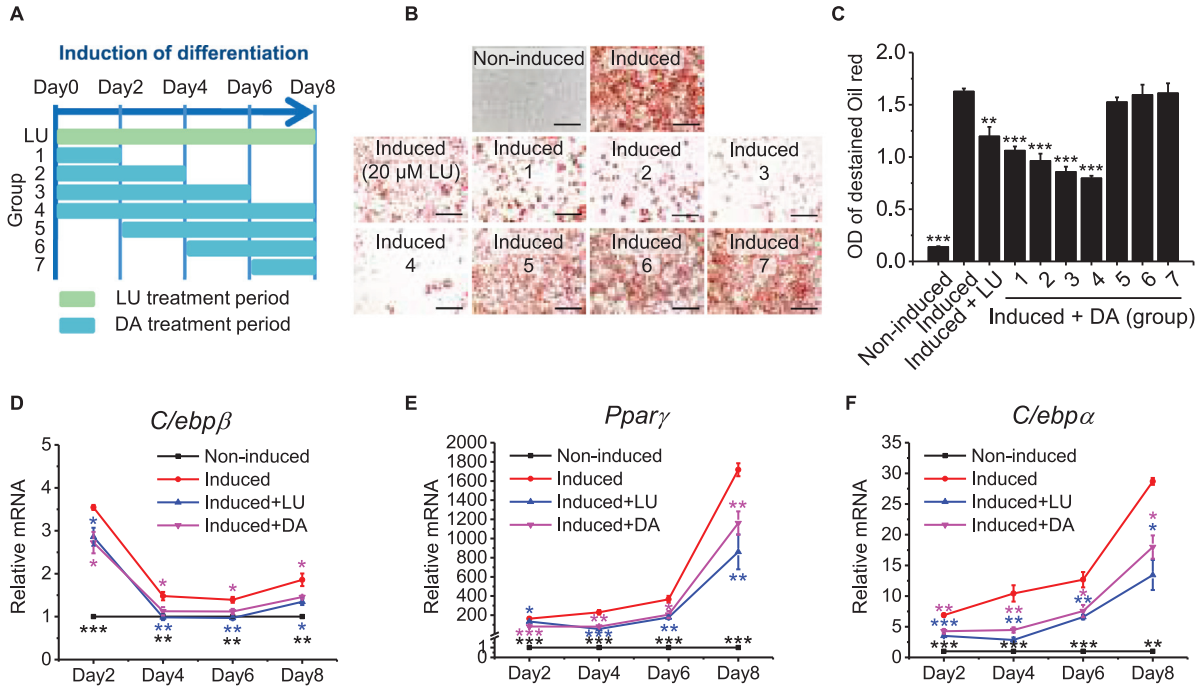

Fig. 2. Effects of DA on the different stages of 3T3-L1 differentiation. (A) The schematic of 23-epi-26-deoxyactein (DA) treatment periods during the differentiation of 3T3-L1 preadipocytes. (B) Oil red O staining of lipid accumulation in differentiated adipocytes. Scale bar, 100 μm. (C) The quantification of Oil red O staining in 3T3-L1 adipocytes ($n = 4$). (D–F) Relative mRNA expression of adipocyte-specific transcription factors *C/ebpβ* (D), *Pparγ* (E), and *C/ebpα* (F) ($n = 4$). All data in (C, D, E, F) are represented as mean ± SEM. Student's *t*-test, * $p < 0.05$, ** $p < 0.01$, *** $p < 0.001$. LU, luteolin.

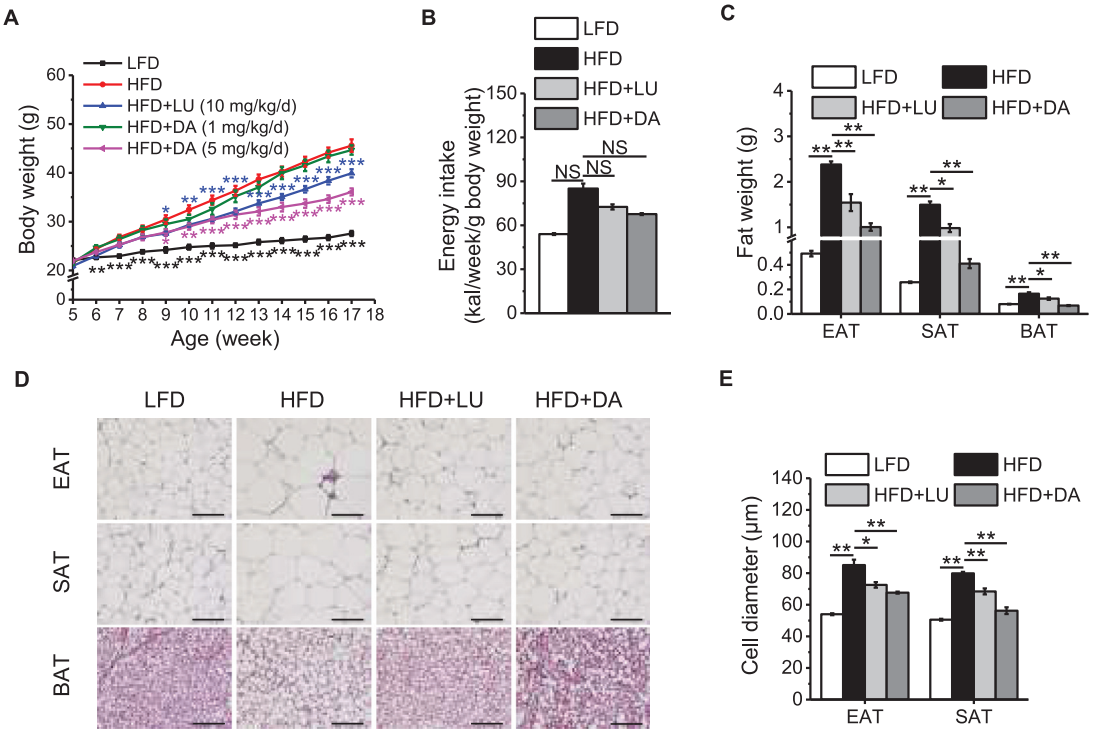

Fig. 3. Effects of DA on diet-induced obesity in mice. (A–C) Bodyweight gain (A), energy intake (B), and adipose tissue weight (C) of mice ($n = 6$–10). (D) Hematoxylin and eosin (H&E) staining of epididymal adipose tissue (EAT), subcutaneous adipose tissue (SAT), and brown adipose tissue (BAT) sections. Scale bar, 100 μm. (E) Adipocyte diameters of EAT and SAT from mice ($n = 6$). All data are represented as mean ± SEM. Statistical difference was determined by Mann-Whitney U test, * $p < 0.05$, ** $p < 0.01$, *** $p < 0.001$, and NS, not significant. LFD, low-fat diet; HFD, high-fat diet; HFD +LU, HFD diet with 10 mg/kg/day luteolin; HFD +DA, HFD diet with 5 mg/kg/day 23-epi-26-deoxyactein.

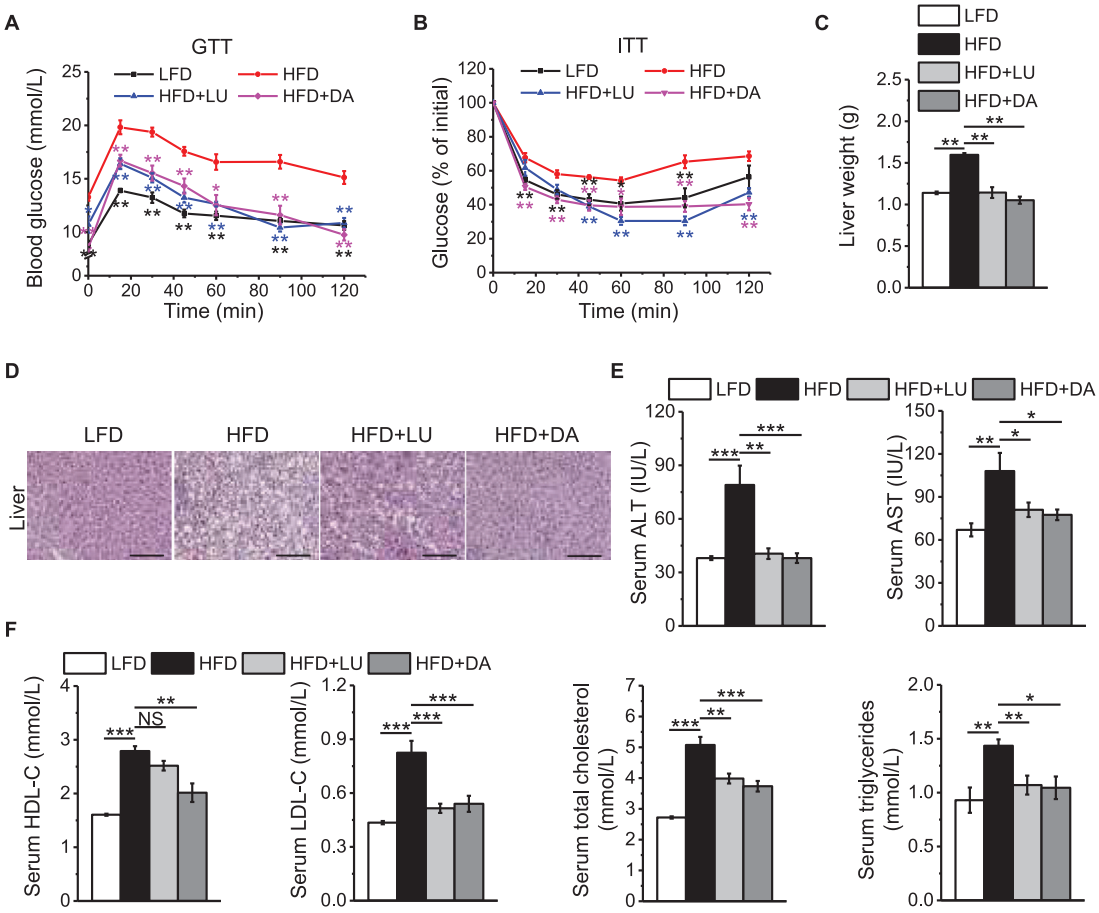

Fig. 4. Effects of DA on obesity-related metabolic disorders in HFD-fed mice. (A, B) The glucose tolerance test (GTT) (A) and insulin tolerance test (ITT) (B) in mice (n = 6). (C) The liver weight of mice (n = 6). (D) H&E staining of liver sections. Scale bar, 100 μm. (E) Serum levels of alanine aminotransferase (ALT) and aspartate aminotransferase (AST) of mice (n = 8). (F) Serum levels of high-density lipoprotein cholesterol (HDL-C), low-density lipoprotein cholesterol (LDL-C), total cholesterol (TC), and total triglyceride (TG) of mice (n = 8). All data are represented as mean ± SEM. Mann-Whitney U test, * $p < 0.05$, ** $p < 0.01$, *** $p < 0.001$, and NS, not significant. LFD, low-fat diet; HFD, high-fat diet; HFD + LU, HFD diet with 10 mg/kg/day luteolin; HFD + DA, HFD diet with 5 mg/kg/day 23-epi-26-deoxyactein.

examined the effects of DA on adipocyte adipogenesis, lipogenesis, and lipolysis, respectively. In 3T3-L1 cells, DA exhibited the potent inhibition of adipogenesis (Figs. 1 and 2). Further, we found that the mRNA levels of lipolysis-related genes, including *Atgl, Hsl*, and *perilipin*, were upregulated by DA in adipose tissue (Fig. 5A). However, interestingly, DA did not down-regulated the expression of lipogenesis-related genes in adipose tissue (Fig. 5B). These observations suggest that DA prevents obesity through inhibiting adipogenesis and promoting lipolysis, rather than reducing lipogenesis.

Adipose tissue is a major site of TG storage. In HFD-induced obesity, excessive fat accumulation in adipocytes causes adipose tissue dysfunction, resulting in the storage of excess lipids into other tissues. As a

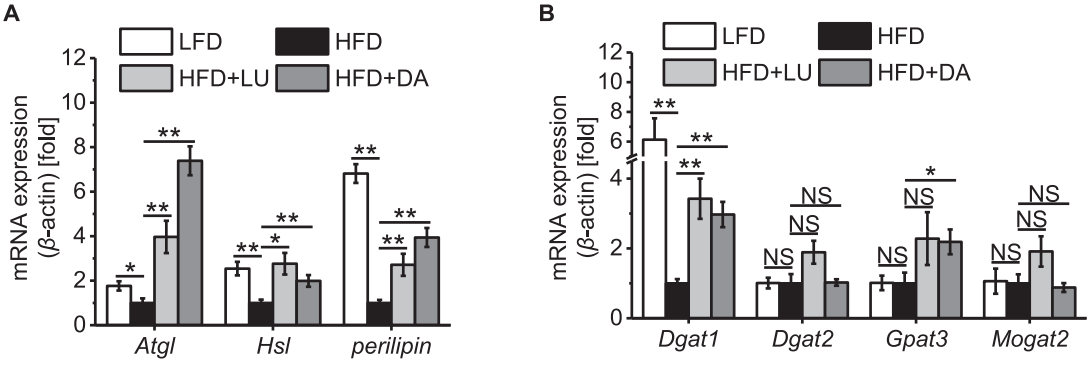

Fig. 5. Effects of DA on lipogenesis and lipolysis in adipose tissue. (A) Relative mRNA expression of lipolysis-related genes in adipose tissue (n = 6). (B) Relative mRNA expression of lipogenesis-related genes in adipose tissue (n = 6). All data are represented as mean ± SEM. Mann-Whitney U test, * $p < 0.05$, ** $p < 0.01$, and NS, not significant. LFD, low-fat diet; HFD, high-fat diet; HFD + LU, HFD diet with 10 mg/kg/day luteolin; HFD + DA, HFD diet with 5 mg/kg/day 23-epi-26-deoxyactein.

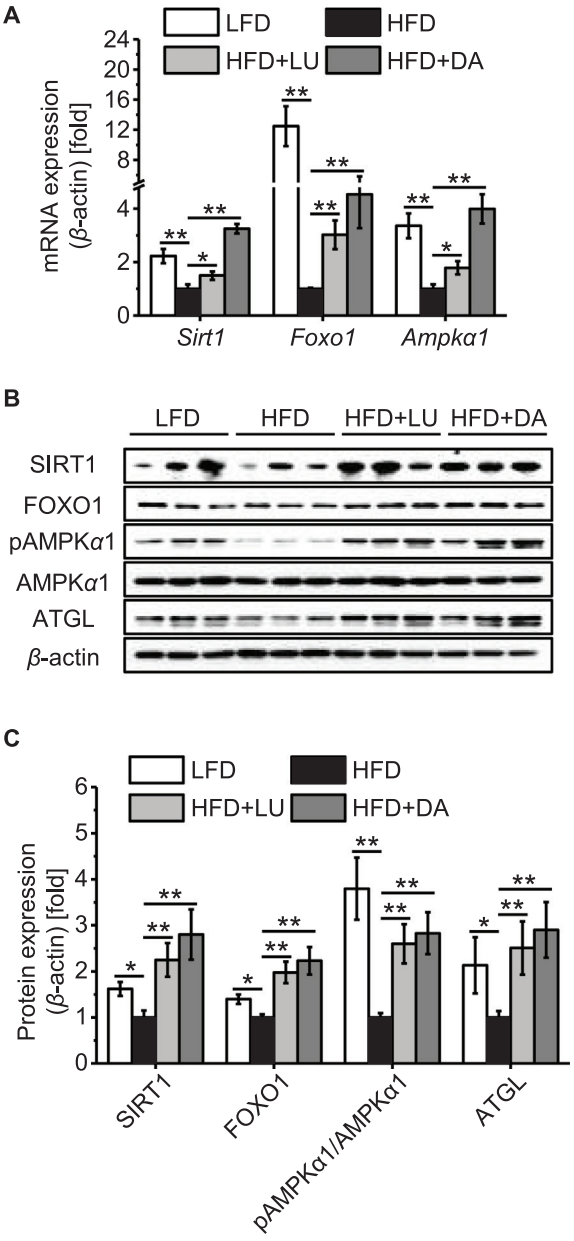

Fig. 6. Effects of DA on AMPK signaling and SIRT1-FOXO1 pathway. (A) Relative mRNA expression of *Sirt1, Foxo1*, and *Ampkα1* in adipose tissue ($n = 6$). (B) Representative western blots of SIRT1, FOXO1, pAMPKα1, AMPKα1, and ATGL in adipose tissue. (C) The densitometry quantification of SIRT1, FOXO1, pAMPKα1/AMPKα1, and ATGL in adipose tissue ($n = 6$). All data in (A, C) are represented as mean ± SEM. Mann-Whitney U test, * $p < 0.05$, ** $p < 0.01$. LFD, low-fat diet; HFD, high-fat diet; HFD + LU, HFD diet with 10 mg/kg/day luteolin; HFD + DA, HFD diet with 5 mg/kg/day 23-epi-26-deoxyactein.

result, the overaccumulation of fat in non-adipose tissues can lead to lipotoxicity-related diseases. For instance, ectopic lipid accumulation in liver is associated with insulin resistance and hepatic steatosis, which plays a crucial role in the pathogenesis of type 2 diabetes and non-alcoholic fatty liver (Samuel and Shulman, 2018). Our study showed that DA not only reduced adipose tissue fat accumulation, but also decreased serum lipids, liver vacuolization, and systemic insulin resistance in HFD-fed mice (Figs. 3 and 4). Indeed, DA also reversed HFD-induced depression on the expression of *Dgat1* (Fig. 5B), which is a rate-limiting enzyme in TG synthesis (Chitraju et al., 2017). These findings suggest that DA protects mice against HFD-induced metabolic alterations through alleviating adipocyte dysfunction.

As the critical nutrient-sensing molecules, AMPK and SIRT1 play multiple roles in regulating lipid metabolism. It has been shown that AMPK could activate ATGL to induce lipolysis (Ahmadian et al., 2011). SIRT1-mediated deacetylation of FOXO1 also elevated ATGL mRNA expression, and SIRT1 silencing inhibited lipolysis in adipocytes (Chakrabarti et al., 2011). Moreover, DA has been reported to promote AMPK activation in HepaRG cells and SIRT1 expression in pancreatic β-cells (Moser et al., 2014; Suh et al., 2017). Here, we found that DA significantly elevated the expression of ATGL, SIRT1, and FOXO1, as well as the phosphorylation of AMPKα1 in adipose tissue (Fig. 6). These results indicate that DA may be a potent activator of AMPK singling and SIRT1-FOXO1 pathway, a hypothesis that merits further investigation.

Conclusion

To our knowledge, DA is the first compound in *A. racemosa* that exhibits a potent anti-obesity activity in 3T3-L1 preadipocytes and HFD-fed mice, although other *A. racemosa* ingredients (*e.g.*, protopine hydrochloride) could also promote AMPK activation in HepaRG cells (Moser et al., 2014). In conclusion our study demonstrates that 10 μM DA suppresses adipogenesis in 3T3-L1 preadipocytes, and 5 mg/kg/d DA ameliorates diet-induced obesity and associated metabolic alterations in mice, suggesting that DA is a promising natural compound for the treatment of obesity and related metabolic diseases.

CRediT authorship contribution statement

Jingjing Yuan: Conceptualization, Investigation, Formal analysis, Writing - original draft, Visualization. **Qiangqiang Shi:** Investigation, Writing - review & editing. **Juan Chen:** Validation. **Jing Lu:** Investigation. **Lu Wang:** Formal analysis. **Minghua Qiu:** Resources, Writing - review & editing, Funding acquisition. **Jian Liu:** Conceptualization, Resources, Writing - review & editing, Project administration, Funding acquisition.

Declaration of Competing Interest

The authors declare no competing financial interest.

Acknowledgments

This work was funded by the National Natural Science Foundations of China (31671485 to J.L., and U1132604 to M.Q.) .

Supplementary materials

Supplementary material associated with this article can be found, in the online version, at doi:10.1016/j.phymed.2020.153264.

References

Ahmadian, M., Abbott, M.J., Tang, T., Hudak, C.S., Kim, Y., Bruss, M., Hellerstein, M.K., Lee, H.Y., Samuel, V.T., Shulman, G.I., Wang, Y., Duncan, R.E., Kang, C., Sul, H.S., 2011. Desnutrin/ATGL is regulated by AMPK and is required for a brown adipose phenotype. Cell Metab. 13, 739–748.

Bornfeldt, K.E., Tabas, I., 2011. Insulin resistance, hyperglycemia, and atherosclerosis. Cell Metab. 14, 575–585.

Chakrabarti, P., English, T., Karki, S., Qiang, L., Tao, R., Kim, J., Luo, Z., Farmer, S.R., Kandror, K.V., 2011. SIRT1 controls lipolysis in adipocytes via FOXO1-mediated expression of ATGL. J. Lipid Res. 52, 1693–1701.

Chang, E., Kim, C.Y., 2019. Natural products and obesity: a focus on the regulation of mitotic clonal expansion during adipogenesis. Molecules 24, 1157–1178.

Chitraju, C., Mejhert, N., Haas, J.T., Diaz-Ramirez, L.G., Grueter, C.A., Imbriglio, J.E., Pinto, S., Koliwad, S.K., Walther, T.C., Farese Jr., R.V., 2017. Triglyceride synthesis by DGAT1 protects adipocytes from lipid-induced ER stress during lipolysis. Cell Metab. 26, 407–418.

Choi, E.M., 2013. Deoxyactein isolated from *Cimicifuga racemosa* protects osteoblastic MC3T3-E1 cells against antimycin A-induced cytotoxicity. J. Appl. Toxicol. 33,

488–494.
Coleman, R.A., Mashek, D.G., 2011. Mammalian triacylglycerol metabolism: synthesis, lipolysis, and signaling. Chem. Rev. 111, 6359–6386.
Committee on Herbal Medicinal Products, 2018. Black cohosh. London: European Medicines Agency. Report no.: EMA/265439/2018.
Cristancho, A.G., Lazar, M.A., 2011. Forming functional fat: a growing understanding of adipocyte differentiation. Nat. Rev. Mol. Cell Biol. 12, 722–734.
Einbond, L.S., Shimizu, M., Xiao, D., Nuntanakorn, P., Lim, J.T., Suzui, M., Seter, C., Pertel, T., Kennelly, E.J., Kronenberg, F., Weinstein, I.B., 2004. Growth inhibitory activity of extracts and purified components of black cohosh on human breast cancer cells. Breast Cancer Res. Treat. 83, 221–231.
Frühbeck, G., Méndez-Giménez, L., Fernández-Formoso, J.A., Fernández, S., Rodríguez, A., 2014. Regulation of adipocyte lipolysis. Nutr. Res. Rev. 27, 63–93.
Hsieh, Y.-H., Wang, S.-Y., 2013. Lucidone from *Lindera erythrocarpa* Makino fruits suppresses adipogenesis in 3T3-L1 cells and attenuates obesity and consequent metabolic disorders in high-fat diet C57BL/6 mice. Phytomedicine 20, 394–400.
Hsu, C.L., Yen, G.C., 2007. Effects of capsaicin on induction of apoptosis and inhibition of adipogenesis in 3T3-L1 cells. J. Agric. Food Chem. 55, 1730–1736.
Kelly, T., Yang, W., Chen, C.S., Reynolds, K., He, J., 2008. Global burden of obesity in 2005 and projections to 2030. Int. J. Obes. 32, 1431–1437.
Kwon, E.Y., Jung, U.J., Park, T., Yun, J.W., Choi, M.S., 2015. Luteolin attenuates hepatic steatosis and insulin resistance through the interplay between the liver and adipose tissue in mice with diet-induced obesity. Diabetes 64, 1658–1669.
Masada-Atsumi, S., Kumeta, Y., Takahashi, Y., Hakamatsuka, T., Goda, Y., 2014. Evaluation of the botanical origin of black cohosh products by genetic and chemical analyses. Biol. Pharm. Bull. 37, 454–460.
Moser, C., Vickers, S.P., Brammer, R., Cheetham, S.C., Drewe, J., 2014. Antidiabetic effects of the *Cimicifuga racemosa* extract Ze 450 *in vitro* and *in vivo* in *ob/ob* mice. Phytomedicine 21, 1382–1389.
NCD Risk Factor Collaboration, 2017. Worldwide trends in body-mass index, underweight, overweight, and obesity from 1975 to 2016: a pooled analysis of 2416 population-based measurement studies in 128•9 million children, adolescents, and adults. Lancet 390, 2627–2642.
Ntambi, J.M., Young-Cheul, K., 2000. Adipocyte differentiation and gene expression. J. Nutr. 130, 3122s–3126s.
Park, H.-S., Kim, S.-H., Kim, Y.S., Ryu, S.Y., Hwang, J.-T., Yang, H.J., Kim, G.-H., Kwon, D.Y., Kim, M.-S., 2009. Luteolin inhibits adipogenic differentiation by regulating PPARγ; activation. BioFactors 35, 373–379.
Rachoń, D., Vortherms, T., Seidlová-Wuttkea, D., Wuttke, W., 2008. Effects of black cohosh extract on body weight gain, intra-abdominal fat accumulation, plasma lipids and glucose tolerance in ovariectomized Sprague-Dawley rats. Maturitas 60, 209–215.
Sam, S., Mazzone, T., 2014. Adipose tissue changes in obesity and the impact on metabolic function. Transl. Res. 164, 284–292.
Samuel, V.T., Shulman, G.I., 2018. Nonalcoholic fatty liver disease as a nexus of metabolic and hepatic diseases. Cell Metab. 27, 22–41.
Suh, K.S., Choi, E.M., Jung, W.W., Kim, Y.J., Hong, S.M., Park, S.Y., Rhee, S.Y., Chon, S., 2017. Deoxyactein protects pancreatic *β*;-cells against methylglyoxal-induced oxidative cell damage by the upregulation of mitochondrial biogenesis. Int. J. Mol. Med. 40, 539–548.
Sun, Y., Yu, Q., Shen, Q., Bai, W., Kang, J., 2016. Black cohosh ameliorates metabolic disorders in female ovariectomized rats. Rejuvenation Res. 19, 204–214.
Tang, Q.Q., Lane, M.D., 2012. Adipogenesis: from stem cell to adipocyte. Annu. Rev. Biochem. 81, 715–736.
Wang, H.-K., Sakurai, N., Shih, C.Y., Lee, K.-H., 2005. LC/TIS-MS fingerprint profiling of *Cimicifuga* species and analysis of 23-epi-26-deoxyactein in *Cimicifuga racemosa* commercial products. J. Agric. Food Chem. 53, 1379–1386.
Wang, Q.A., Tao, C., Gupta, R.K., Scherer, P.E., 2013. Tracking adipogenesis during white adipose tissue development, expansion and regeneration. Nat. Med. 19, 1338–1344.
World Health Organization. Obesity and overweight. https://www.who.int/en/news-room/fact-sheets/detail/obesity-and-overweight (accessed, 15 April 2020).
Xu, N., Zhang, L., Dong, J., Zhang, X., Chen, Y.G., Bao, B., Liu, J., 2014. Low-dose diet supplement of a natural flavonoid, luteolin, ameliorates diet-induced obesity and insulin resistance in mice. Mol. Nutr. Food Res. 58, 1258–1268.
Zechner, R., Zimmermann, R., Eichmann, T.O., Kohlwein, S.D., Haemmerle, G., Lass, A., Madeo, F., 2012. Fat signals - lipases and lipolysis in lipid metabolism and signaling. Cell Metab. 15, 279–291.
Zhang, X., Zhang, Q.X., Wang, X., Zhang, L., Qu, W., Bao, B., Liu, C.A., Liu, J., 2016. Dietary luteolin activates browning and thermogenesis in mice through an AMPK/PGC1α; pathway-mediated mechanism. Int. J. Obes. 40, 1841–1849.